

# Anisotropic thermal expansion of oriented crystalline polymers

C.L. Choy, F.C. Chen and E.L. Ong

Department of Physics, Chinese University of Hong Kong, Hong Kong

The linear thermal expansivity of oriented high-density polyethylene (HDPE) and polypropylene (PP) with draw ratio between 1 and 18 has been measured between 120 and 300 K. The expansivity perpendicular to the draw direction  $\hat{z}$  ( $\alpha_{\perp}$ ) increases with  $\lambda$ , because of the alignment of the crystallite chain axes along  $\hat{z}$ ; the expansivity parallel to  $\hat{z}$  ( $\alpha_{\parallel}$ ) decreases very sharply with  $\lambda$ , becoming negative at about  $\lambda = 3$  for HDPE and  $\lambda = 7$  for PP — a consequence of the negative expansivity of the crystalline phase along its chain axis and the constraining effect of the stiff intercrystalline bridges. A model treating the drawn crystalline polymer as a composite consisting of partly aligned crystallites embedded in an isotropic amorphous matrix is adequate for explaining the behaviour of  $\alpha_{\perp}$ , whereas a parallel-series model can give reasonable estimates of  $\alpha_{\parallel}$  for ultra-oriented samples, which is largely independent of  $\lambda$  and decreases with increasing temperature. However, neither model can account for the behaviour of  $\alpha_{\parallel}$  at low draw ratio.

## INTRODUCTION

When a semicrystalline polymer is uniaxially oriented it exhibits a rapid increase in both the tensile modulus<sup>1-9</sup> and thermal conductivity<sup>10-14</sup> along the draw direction but only a slight decrease in these quantities along the perpendicular direction. This anisotropy can be attributed to two major factors: the alignment of the covalently bonded chains in the crystalline blocks along the draw direction, and the increase in the volume fraction  $\nu_f$  of intercrystalline bridges formed during the drawing process. The orientation of the crystalline blocks is described by the function  $f_c$  which increases rapidly and reaches a value of about 0.9 at a draw ratio  $\lambda = 5$ , above which its effect will soon become saturated; in contrast,  $\nu_f$  continues to increase up to the highest draw ratio attainable, so they are mainly responsible for the extremely large anisotropy produced at high draw ratio. In case of high-density polyethylene (HDPE) the anisotropy reaches 60 at  $\lambda = 25$ .<sup>13,14</sup>

The thermal expansion of oriented polymers also shows anisotropy. Hellwege *et al.*<sup>15</sup> have studied amorphous polymers and found that the linear thermal expansivity along the draw direction ( $\alpha_{\parallel}$ ) decreases with  $\lambda$  while the expansivity perpendicular to that direction ( $\alpha_{\perp}$ ) increases. The anisotropy  $A = \alpha_{\parallel}/\alpha_{\perp}$  is strongly dependent on material: it is 1.1 and 2.5 at  $\lambda = 4$  for polystyrene (PS) and polymethyl methacrylate (PMMA), respectively; for polyvinyl chloride (PVC), which probably has a crystallinity of about 0.1,  $A$  goes up to 4.5 even at  $\lambda = 3$ .

This led us to the expectation that the anisotropy might be even larger for highly crystalline polymers such as HDPE and polypropylene (PP). At room temperature, the expansivity of the crystallite of PE obtained from x-ray diffraction experiments<sup>16,17</sup> are  $\alpha_{\perp}^c = 13 \times 10^{-5} \text{ K}^{-1}$  and  $\alpha_{\parallel}^c = -1.3 \times 10^{-5} \text{ K}^{-1}$ , and the expansivity of the amorphous region  $\alpha^a$  is about  $30 \times 10^{-5} \text{ K}^{-1}$ .<sup>18</sup> So, assuming a series arrangement of the two regions, we expect a fully oriented sample of crystallinity  $\nu = 0.8$  to have  $\alpha_{\parallel} = \nu\alpha_{\parallel}^c + (1 - \nu)\alpha^a \simeq 5 \times 10^{-5} \text{ K}^{-1}$ . However, Porter and coworkers<sup>19,20</sup> found that  $\alpha_{\parallel}$  of highly extruded PE ( $\lambda \sim 46$ ) has a negative value

( $\simeq -1.0 \times 10^{-5} \text{ K}^{-1}$ ), which differs from  $\alpha_{\parallel}^c$  by only 30%.

It is thus clear that for such an ultraoriented sample the intercrystalline bridges play a dominant role in determining expansivity, probably by constraining the expansion of the amorphous region along the draw direction.

To obtain a better understanding of the various factors which determine the expansivity of oriented polymers, it is essential to have more complete data with regard to both draw ratio  $\lambda$  and temperature  $T$ , and to compare them with calculations wherever possible. We have therefore measured  $\alpha_{\perp}$  and  $\alpha_{\parallel}$  of HDPE and PP between  $\lambda = 1$  and 18, and from 120 to 300 K. The results show very remarkable features in both  $\lambda$  and  $T$  dependence, and can be understood to a certain extent using crude models based on morphological changes indicated by recent investigations.

## THEORETICAL CONSIDERATIONS

The effect of orientation on the morphology of high-density polyethylene (HDPE) has been extensively studied,<sup>21-25</sup> and a brief description of the relevant features would be helpful to the analysis of the present work.

The isotropic sample consists of crystalline lamellae (thickness 100–400 Å) embedded in an amorphous matrix.<sup>41</sup> Each lamella is composed of mosaic crystalline blocks of lateral dimension 100–200 Å with boundaries defined by dislocations.<sup>26</sup> The lamellae are randomly oriented, and generally arrange themselves end-to-end in ribbon-like structures, which grow out from nucleating centres to form spherulites. As polyethylene is oriented the crystalline orientation function  $f_c$  increases rapidly and reaches 0.9 at  $\lambda = 5$ . The spherulitic structure is deformed and broken up, and the crystalline blocks are pulled out of the lamellae. On further deformation these blocks will align along the draw direction, forming fibrillar stacks of chain-folded crystallites, which are connected by intercrystalline bridges (regarded as crystalline material). Alternatively, the ultra-oriented sample can be regarded as a continuous crystal

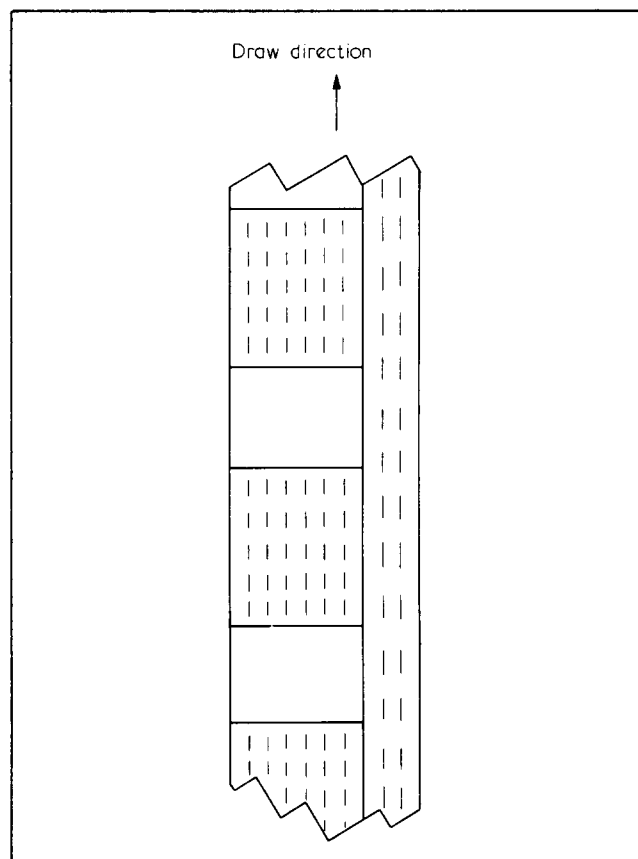


Figure 1 Schematic diagram showing the structure of a highly oriented semicrystalline polymer. The blank areas denote the amorphous regions while the dashed lines represent the chain axes in the crystalline regions.

containing disordered regions which are periodic in the draw direction, as shown schematically in Figure 1.

Recently Gibson *et al.*<sup>25</sup> found that as  $\lambda$  increases from 5 to 30 the lateral dimension (about 110 Å) and the long period (about 200 Å) of this structure remain unchanged, whereas the average crystal length  $\bar{D}_{002}$  increases from 228 to 464 Å along the  $\hat{c}$ -direction, implying an increase in crystal continuity throughout this range of  $\lambda$ . The structure of oriented polypropylene has not received as much attention, but it may be similar to PE.

From the above account it is seen that the drawn polymer can be expected to have quite different behaviour at low and high draw ratio, with  $\lambda = 5$  as the approximate dividing line. Simple models will now be described which allow us to make rough calculations of the expansivity in these two regions.

#### Low draw ratio

At low draw ratio the intercrystalline bridges might be negligible, so the drawn polymer may be regarded as a two-phase composite consisting of crystalline blocks (which may or may not have been pulled out of the lamellae) embedded in an amorphous matrix. The drawing process mainly increases the alignment of the crystalline chain axes of these blocks along the draw direction. Rosen and Hashin<sup>27</sup> derived a general formula for a two-phase composite with fully oriented inclusions, allowing for the most general anisotropy in both thermal and mechanical properties of each phase. However, the formula requires a knowledge of the complete compliance tensors of both phases, and of the composite itself as well. Since complete experimental

data is not available on all the compliances of the crystalline phase and the compliance of a composite with fully oriented anisotropic inclusions at high concentration cannot be calculated, the adaptation of this formula would be difficult.

Consequently, for a rough estimate, assume that the expansivity tensor of a composite  $\alpha'_{ij}$  can be obtained by linear interpolation between those of its component phases when the inclusions are fully aligned, ie

$$\alpha'_{ij} = \nu \alpha_{ij}^c + (1 - \nu) \delta_{ij} \alpha^a \quad (1)$$

where  $\nu$  is the volume fraction crystallinity, and  $\alpha_{ij}^c$  (which is diagonal, with elements  $(\alpha_{\perp}^c, \alpha_{\perp}^c, \alpha_{\parallel}^c)$ ) and  $\delta_{ij} \alpha^a$  are the expansivity tensor of the crystalline and the (isotropic) amorphous phase, respectively. Since this expression must be correct for  $\nu = 0$  and  $\nu = 1$ , its application to a highly crystalline ( $\nu = 0.6-0.8$  in our case) polymer would not be unreasonable. Furthermore, it is also valid if the matrix behaves like a liquid. This situation is approached above the major transitions, where the shear modulus of the amorphous phase drops to very low values.

Taking the distribution in the chain alignment of the crystalline blocks into account, the weighted average of the tensor  $\alpha'_{ij}$  over the solid angle is taken to obtain the expansivity tensor  $\alpha_{ij}$  of the oriented polymer:

$$\alpha_{ij} = \frac{1}{4\pi} \int d\Omega P(\hat{c}) R_{ik}(\hat{c}) R_{jl}(\hat{c}) \alpha'_{kl} \quad (2)$$

where  $P(\hat{c})$  is the distribution of the crystal chain-axis  $\hat{c}$  and  $R_{ik}(\hat{c})$  is the transformation matrix rotating  $\hat{z}$  (the draw-direction) to  $\hat{c}$ . Assuming  $P(\hat{c})$  is symmetrical with respect to  $\hat{z}$  and substituting the actual elements of  $R_{ik}(\hat{c})$  and also equation (1) into equation (2), it is found that  $\alpha_{ij}$  is diagonal and has elements  $(\alpha_{\perp}, \alpha_{\perp}, \alpha_{\parallel})$ , where  $\alpha_{\perp}$  and  $\alpha_{\parallel}$  are the expansivities of the composite perpendicular and parallel to  $\hat{z}$ , respectively:

$$\alpha_{\perp} = \nu \alpha^c + (1 - \nu) \alpha^a + \frac{1}{3} \nu f_c(\lambda) (\alpha_{\perp}^c - \alpha_{\parallel}^c) \quad (3)$$

$$\alpha_{\parallel} = \nu \alpha^c + (1 - \nu) \alpha^a - \frac{2}{3} \nu f_c(\lambda) (\alpha_{\perp}^c - \alpha_{\parallel}^c) \quad (4)$$

Here  $\alpha^c = \frac{1}{3}(2\alpha_{\perp}^c + \alpha_{\parallel}^c)$  is the average expansivity of crystallites, and the distribution function  $f_c(\lambda)$  is  $\frac{1}{2}(3\cos^2\theta - 1)$ ,  $\cos\theta$  being  $\hat{c} \cdot \hat{z}$ .

We note that  $f_c = 0$  for the isotropic sample, in which case both equations (3) and (4) reduce to

$$\alpha_{\text{iso}} = \nu \alpha^c + (1 - \nu) \alpha^a \quad (5)$$

From equations (3) and (4) it is clear that the average expansivity  $\alpha$  for the oriented sample, defined as  $\frac{1}{3}(2\alpha_{\perp} + \alpha_{\parallel})$  or  $1/3$  the volume expansivity, is independent of draw ratio and just equals the isotropic value  $\alpha_{\text{iso}}$ . It is also clear that the  $\lambda$ -dependence of the expansivities arise solely from the partial alignment of  $\hat{c}$  along  $\hat{z}$ , as described by  $f_c(\lambda)$ . This effect becomes saturated when nearly all the crystalline blocks become oriented ( $f_c \approx 1$ ), as is the case for  $\lambda > 5$ . Then  $\alpha_{\perp, \parallel}$  becomes independent of  $\lambda$ , and in any case the appearance of intercrystalline bridges would render equations (3) and (4) inapplicable.

#### High draw ratio

Various models<sup>9,13,25,28</sup> have been proposed to explain the high mechanical stiffness and thermal conductivity of the

ultra-oriented polymer on the basis of simplified pictures of the morphology. Among these the recent work of Gibson *et al.*<sup>25</sup> is particularly attractive, in that it is based on wide- and low-angle X-ray diffraction and contains no arbitrary parameter. By statistical considerations they suggest that the volume fraction  $v_f$  of the interconnecting crystalline fibres (or intercrystalline bridge material) is  $v_f = vp(2 - p)$ , where  $p$  is the probability of a chain within a crystallite traversing the intervening disordered region and entering the next crystallite on the stack.  $p$  can be obtained from the observed average crystal length  $\bar{D}_{002}$  and the long period  $L$  through the relation  $\bar{D}_{002} = L(1 + p)/(1 - p)$ , and its value for different  $\lambda$  has been tabulated for drawn and extruded HDPE.<sup>25</sup>

It is now straightforward to apply the schematic diagram shown in *Figure 1* to the calculation of expansivity. In this scheme the chain-folded crystalline block thermally expands in series with the amorphous region along the draw direction, but the entire stack is constrained by the intercrystalline bridges in parallel with it. The sequence of series-parallel connection is reversed in the perpendicular direction. A simple calculation leads to the following results, which have previously been derived by Capiati and Porter:<sup>20</sup>

$$\alpha_{\perp} = \alpha_{\perp}^c + \frac{\alpha^a - \alpha_{\perp}^c}{\eta + 1} \quad (6)$$

$$\alpha_{\parallel} = \alpha_{\parallel}^c + q(\alpha^a - \alpha_{\parallel}^c) \quad (7)$$

where

$$\eta = \frac{v - v_f}{1 - v} \frac{E_{\perp}^c}{E^a}, \quad q = \left[ (1 - v)^{-1} + v_f(1 - v_f)^{-1} \left( \frac{E_{\parallel}^c}{E^a} - 1 \right) \right]^{-1},$$

$E^a$ ,  $E_{\perp}^c$ ,  $E_{\parallel}^c$  being the Young's modulus of the amorphous region, and of the crystalline region perpendicular and parallel to the  $c$ -axis, respectively.

The  $\lambda$ -dependence of  $\alpha_{\perp}$  and  $\alpha_{\parallel}$  as given by equations (6) and (7) is not very strong. In general,  $E_{\parallel}^c/E^a \gg 1$ , therefore  $q \ll 1$  and the constraining effect of the intercrystalline bridges then becomes predominant. In fact, it turns out that when  $\lambda > 7$   $\alpha_{\parallel}$  of PE at room temperature is within 30% of  $\alpha_{\parallel}^c$ . On the other hand,  $\alpha^a$  and  $\alpha_{\perp}^c$  are not very different even at high temperature, therefore  $\alpha_{\perp}$  is again not sensitive to  $\lambda$ , which can affect it through the slowly varying factor  $(v - v_f)$  in  $\eta$ .

## EXPERIMENTAL

Isotropic sheets of thickness 8 mm were prepared by compression-moulding of pellets of PE (Rigidex 50) and PP (Hostalen PPK 1060) at about 30 K above their respective melting points. The PE sheets were slowly cooled to 383 K and then quenched to room temperature while the PP sheets were quenched to room temperature directly from the melt. Dumb-bell shaped samples of width 12 mm and gauge length 15 mm were cut from these sheets and drawn to various draw ratios by using an Instron tensile machine.

The PE samples were drawn at 353 K. For  $\lambda < 5$  the drawing rate varies from 2 to 5 mm/min while for higher  $\lambda$  a drawing rate of 20 mm/min was used. Draw ratios from 1 to 18 were obtained by varying the drawing time.<sup>4</sup>

The PP samples were drawn at 398 K and similar procedure as above was used for  $\lambda < 5$ . To obtain samples of higher  $\lambda$  we followed a two-stage drawing process suggested by Taylor and Clark.<sup>8</sup> The samples were first drawn at

50 mm/min (i.e. less than 6% per min) to their final length.

After drawing, the samples were slowly cooled to room temperature and stored for three days to allow for any relaxation in dimensions. The density of each sample was measured by the flotation method. The volume fraction crystallinity  $v$ , given in *Table 1*, was calculated by assuming that the density of the amorphous and crystalline regions are 0.855 g cm<sup>-3</sup> and 1.000 g cm<sup>-3</sup> for PE and 0.854 g cm<sup>-3</sup> and 0.935 g cm<sup>-3</sup> for PP. Except for the PP sample with  $\lambda = 18$  the crystallinity changes very little on drawing, so, in our analysis, the crystallinity is taken to be 0.81 and 0.63 for PE and PP, respectively. Since the PP sample with  $\lambda = 18$  appears white and silky its low density is probably due to the presence of microvoids. Samples for measurements were normally cut into cubes of side 3.5 mm and the 6 surfaces were polished. For highly drawn samples one or two dimensions of the samples could be as small as 1.8 mm.

The thermal expansion measurements were made on a Perkin-Elmer thermomechanical analyser TMS II. The loading used was 4.5 g, which is slightly higher than the true zero loading ( $\sim 4.0$  g) necessary for compensating for the probe buoyancy. With liquid nitrogen as coolant and helium as the gas for heat exchange, the sample was cooled at 10 K/min to 105 K. When equilibrium was reached measurements up to 300 K were made by heating at 10 K/min and simultaneously monitoring on a two-pen recorder the length  $L$  and the temperature  $T$  as sensed by a Chromel-Alumel thermocouple located close to the sample. The  $L$  versus  $T$  curves were reproducible to within 3%.

To compute the expansivity  $\alpha$  from the recorder traces we make use of the method of the moving arc. First, the length  $L$  and temperature  $T$  were read off the trace at 5 K intervals, resulting in a set of 30–40 data points  $(L_i, T_i)$ ,  $(i = 1, 2, \dots, N)$ . A second-order polynomial  $f(T)$  in  $T$  is least-squares fitted to seven consecutive points (say  $i = n - 3, \dots, n, \dots, n + 3$ ) and the expansivity of the centre point ( $i = n$ ) is taken to be  $\alpha_i = (df/dT)/L_0$ , where  $L_0$  is simply taken to be the sample length at room temperature, as its fractional change is extremely small. The 'fitted arcs' obtained from the first seven ( $i = 1, 2, \dots, 7$ ) and last seven points ( $i = N - 6, N - 5, \dots, N$ ) are also used for computing the expansivities of the first four ( $i = 1, \dots, 4$ ) and last four ( $i = N - 3, \dots, N$ ) points, respectively. The results so obtained show some scatter (4–5%), which is not significant to the analysis of our data. Therefore one

*Table 1.* Density and crystallinity of samples

High density polyethylene			Polypropylene		
Draw ratio	Density (g/cm <sup>3</sup> )	Crystallinity	Draw ratio	Density (g/cm <sup>3</sup> )	Crystallinity
1	0.973	0.81	1	0.905	0.63
1.3	0.973	0.81	1.5	0.906	0.64
1.65	0.973	0.81	2.1	0.906	0.64
1.9	0.972	0.81	2.7	0.906	0.64
2.5	0.969	0.78	4	0.907	0.65
3.0	0.967	0.77	5.5	0.906	0.64
3.7	0.965	0.76	6.5	0.905	0.63
5.5	0.967	0.77	8.5	0.905	0.63
7.5	0.967	0.77	11.5	0.905	0.63
11	0.968	0.78	13.5	0.904	0.62
18	0.966	0.77	18	0.889	0.43

smooth curve drawn through the data points  $\alpha_i$  is used as the result of the experiment.

The above measurement procedure and analysis were checked by using a standard aluminium sample and the results were found to be within 7% of the values given in literature.<sup>29</sup> This was taken to be the accuracy of our measurements for samples with expansivity  $\alpha$  larger than  $10^{-5}$ . The uncertainty became larger for smaller expansivity and was estimated to be about 30% for  $\alpha \leq 10^{-6}$ .

The data for  $\alpha_{||}$  presented in the next section were the average of two separate measurements. To ascertain that the drawn samples were transversely isotropic,  $\alpha_{\perp}$  measurements were made both along the thickness and width. The results agree to within the experimental error (7%) and so the average was taken.

## RESULTS AND DISCUSSIONS

The expansivities  $\alpha_{\perp}$  and  $\alpha_{||}$  are plotted against temperature at various draw ratios in Figures 2-5. Since the  $\alpha_{\perp}$  curves for different samples overlap one another only a few of them are shown at widely separated  $\lambda$ , so as to avoid confusion. The most important feature is that  $\alpha_{||}$  decreases very rapidly with  $\lambda$  at all temperatures, becoming negative at  $\lambda \approx 3$  for PE and at  $\lambda \approx 7$  for PP, while  $\alpha_{\perp}$  exhibits only a slight increase. At  $\lambda = 18$   $\alpha_{||}$  of PE is within 30% of  $\alpha_{||}^c$  at 120 K and within 10% of  $\alpha_{||}^c$  above 240 K. For PE  $\alpha_{\perp}$  seems to have attained the highest value at  $\lambda = 5.5$  and at higher  $\lambda$  even shows a slight decrease (see Figures 2 and 7),

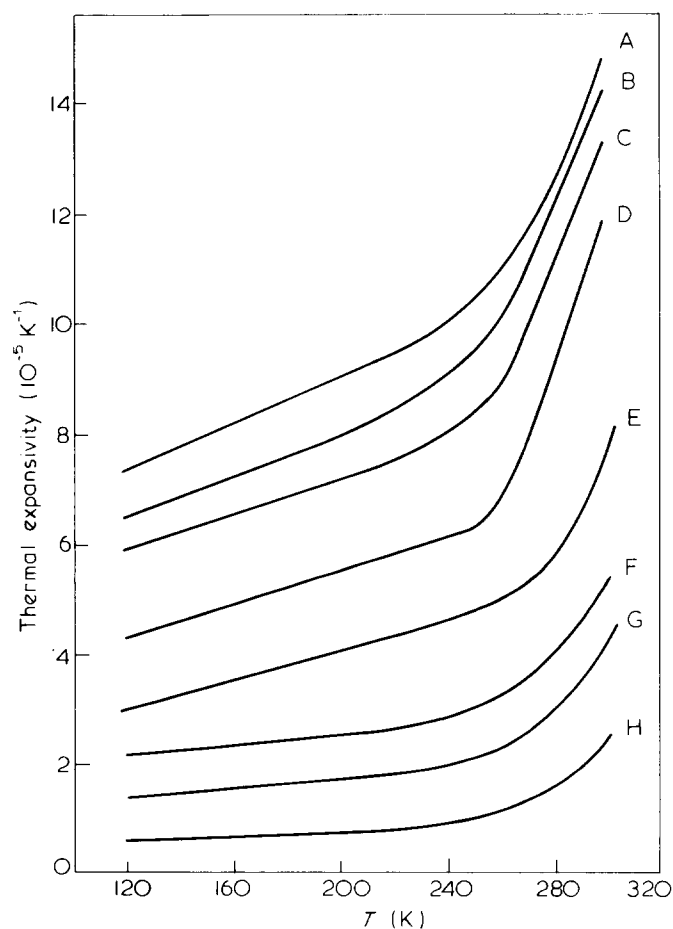


Figure 2 Temperature dependence of the linear thermal expansivities of drawn polyethylene.  $\alpha_{\perp}$ : A,  $\lambda = 5.5$ ; B,  $\lambda = 18$ ; C,  $\lambda = 1.9$ ; D,  $\lambda = 1.3$ .  $\alpha_{||}$ : E,  $\lambda = 1$ ; F,  $\lambda = 1.3$ ; G,  $\lambda = 1.65$ ; H,  $\lambda = 1.9$

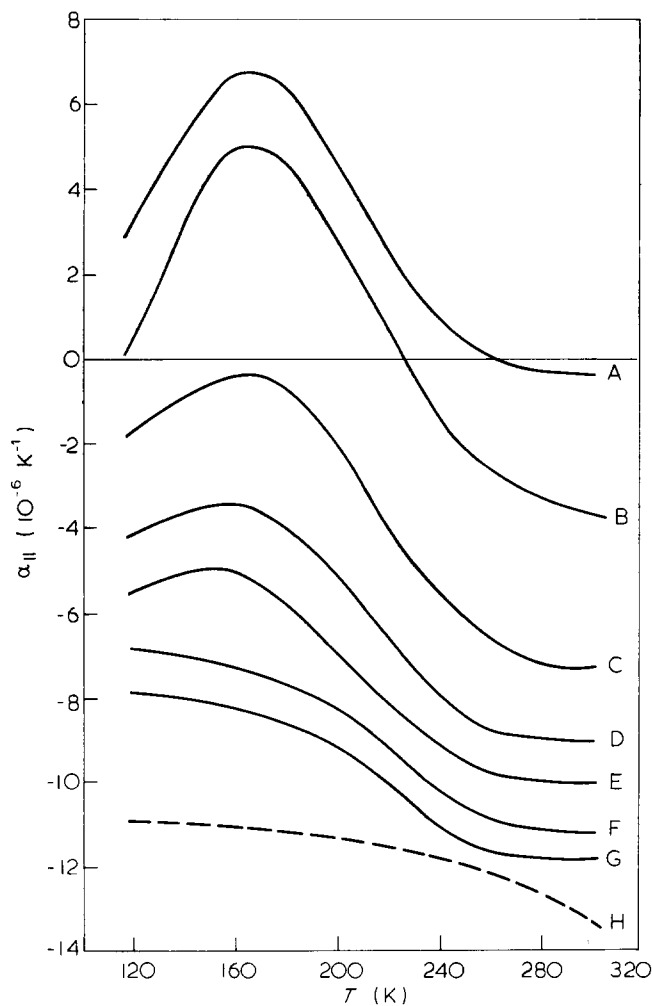
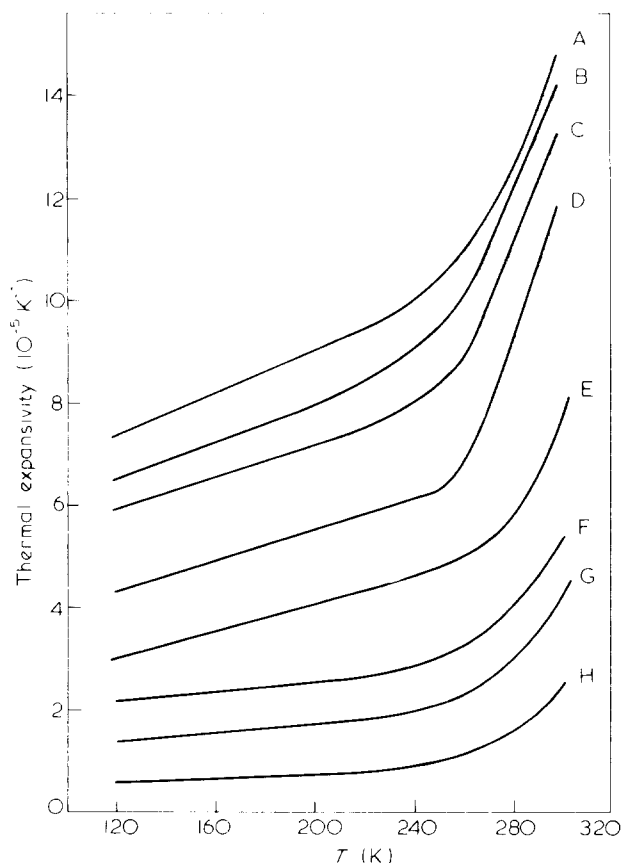


Figure 3 Temperature dependence of  $\alpha_{||}$  of drawn polyethylene. A,  $\lambda = 2.5$ ; B,  $\lambda = 3$ ; C,  $\lambda = 3.7$ ; D,  $\lambda = 5.5$ ; E,  $\lambda = 7.5$ ; F,  $\lambda = 11$ ; G,  $\lambda = 18$ ; H:  $\alpha_c$

which however is within the experimental error (7%) and may not be genuine.

The temperature dependence is different for the two polymers. For PE  $\alpha_{iso}$  and  $\alpha_{\perp}$  show smooth monotonic increases with temperature, whereas in the range  $\lambda = 1.65$  to  $7.5$   $\alpha_{||}$  exhibits a peak near 170 K and a large drop between 170 and 250 K. At higher  $\lambda$  the peak disappears but the large drop persists. For PP there is a sudden increase in expansivity at the glass transition temperature (260 K) in all measurements, except for  $\alpha_{||}$  at  $\lambda > 8$ , which decreases smoothly over the entire temperature range.

Most of these features can be understood on the basis of the models we have developed. First, however, the thermo-mechanical parameters needed for such calculations must be obtained. The orientation functions  $f_c(\lambda)$  for both PE<sup>30</sup> and PP<sup>31</sup> are readily available in literature. The expansivities  $\alpha_{\perp}^c$  and  $\alpha_{||}^c$  of the crystalline phase of PE can be computed from the lattice parameters obtained from x-ray diffraction measurements.<sup>17</sup> The expansivity of the amorphous phase,  $\alpha^a$ , can be obtained by linear extrapolation of the Stehling and Mandelkern data<sup>18</sup> on  $\alpha_{iso}$  at various crystallinities  $\nu$  between 0.57 and 0.84, with the previously extracted average expansivity  $\alpha^c = \frac{1}{3}(2\alpha_{\perp}^c + \alpha_{||}^c)$  for the crystalline phase as a data point for  $\nu = 1$ . The expansivities thus extracted are plotted against temperature in Figure 6.



**Figure 4** Temperature dependence of the linear thermal expansivities of drawn polypropylene.  $\alpha_{\perp}$ : A,  $\lambda = 18$ ; B,  $\lambda = 4$ ; C,  $\lambda = 1.5$ .  $\alpha_{\parallel}$ : D,  $\lambda = 1$ ; E,  $\lambda = 1.5$ ; F,  $\lambda = 2.1$ ; G,  $\lambda = 2.7$ ; H,  $\lambda = 4$

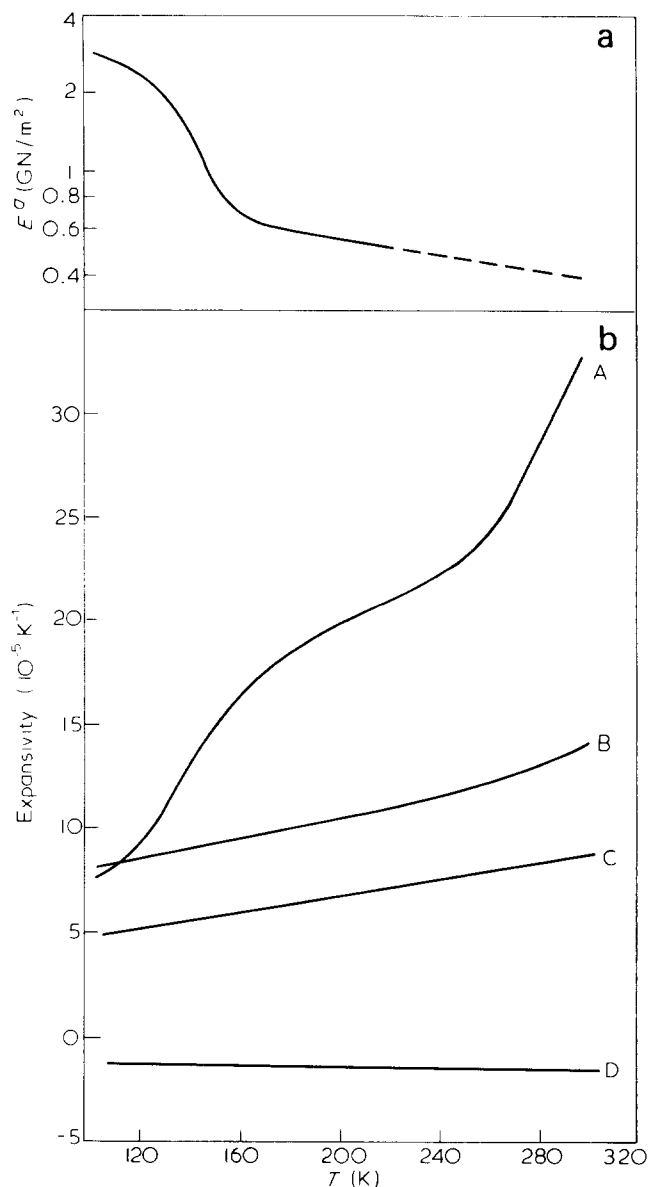


**Figure 6** Temperature dependence of a- $E^a$ ; b-the linear thermal expansivities of the amorphous and crystalline regions of polyethylene. Dashed curve: extrapolation of  $E^a$  to high temperature A:  $\alpha^a$ ; B:  $\alpha_{\perp}^c$ ; C:  $\alpha^c$ ; D:  $\alpha_{\parallel}^c$ .

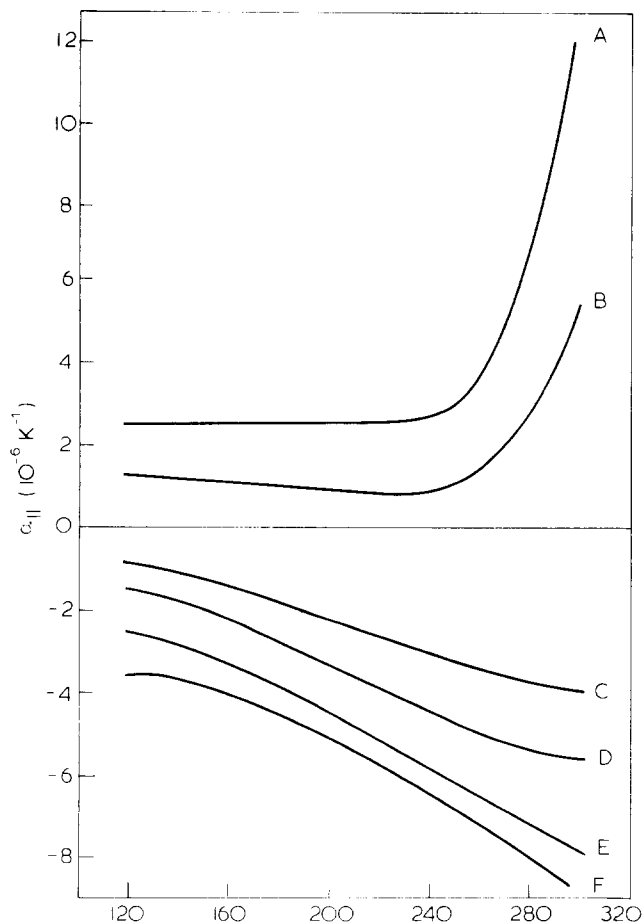


**Figure 5** Temperature dependence of  $\alpha_{\parallel}$  of drawn polypropylene. A,  $\lambda = 5.5$ ; B,  $\lambda = 6.5$ ; C,  $\lambda = 8.5$ ; D,  $\lambda = 11.5$ ; E,  $\lambda = 13.5$ ; F,  $\lambda = 18$

As for PP, the only measurement available is  $\alpha_{\text{iso}}$  as a function of  $\nu$ ,<sup>32</sup> from which  $\alpha^a$  and  $\alpha^c$  can be deduced by linear extrapolation at a few temperatures. In the absence of any further information on  $\alpha_{\perp}^c$  and  $\alpha_{\parallel}^c$ , we assume that at 280 K  $\alpha_{\parallel}^c \approx -1.0 \times 10^{-5}/\text{K}$ , which is slightly less than the observed value of  $\alpha_{\parallel}$  for the most highly drawn sample ( $\lambda = 18$ ), and about the same as the corresponding value for PE. Making the further assumption that its temperature coefficient is the same as that for PE,  $\alpha_{\parallel}^c$  can be estimated at 120 K and 240 K, and the corresponding values of  $\alpha_{\perp}^c$  may be deduced from  $\alpha^c$ . The results are tabulated in Table 2.

Analysis of the ultra-oriented samples requires a knowledge of  $\nu_f$  and hence can only be carried out for PE, for which the determination of  $p$  by Gibson *et al.*<sup>25</sup> is available, yielding values of  $\nu_f$  between 7 and 46% as  $\lambda$  varies from 5.5 to 18.  $E_{\parallel}^c$  and  $E_{\perp}^c$  are assumed to be independent of temperature and equal 255 and 4 GN/m<sup>2</sup>, respectively.<sup>33-36</sup>  $E^a$  can be deduced from the value of  $G^a$  (shear modulus of

the amorphous phase) obtained through extrapolation by Gray and McCrum.<sup>37</sup> This is done by assuming a reasonable value for Poisson's ratio ( $\nu = 0.5$ ), leading to values of  $E^a$  shown in Figure 6. We have verified that the final results are not sensitive to the value of Poisson's ratio as long as it is within the range 0.3–0.5.

In Figures 7a–c the data on  $\alpha_{\parallel}$ ,  $\alpha_{\perp}$  and  $\alpha$  for PE are shown alongside the predictions of equations (3) and (4) at three convenient temperatures: 120 K (below the  $\gamma$ -transition at 145 K), 170 K (just above the  $\gamma$ -transition) and 280 K. It is seen that there is fairly good agreement between data and theory for  $\alpha_{\perp}$  and  $\alpha$  even up to very high draw ratios, which is not too surprising since both quantities are not expected to be sensitive to the appearance of intercrystalline bridges. In particular, the predicted  $\lambda$ -independence of the average expansivity  $\alpha$  seems to hold. On the other hand, the agreement is poor for  $\alpha_{\parallel}$ , which has a very fast drop at low draw ratio that cannot be accounted for by the model. This may reflect a failure of the linear mixing rule, equation (1), because of high mechanical anisotropy, or may be due to the presence of a small amount of intercrystalline bridge material which can very effectively constrain the expansion.

The predictions of the model for ultra-oriented samples as given by equation (6) and (7) are plotted on the same graphs. Since there is no adjustable parameter in the calculation, the agreement with data is quite impressive. For  $\alpha_{\parallel}$  this merely shows that the constraining effect of the intercrystalline bridges has already been saturated, so the result approaches  $\alpha_{\parallel}^c$  and becomes insensitive to  $\nu_f$ . Equally good fits can be achieved if the experimentally determined values of  $\nu_f$  are changed by as much as 50%. It is noted that the measurements of Buckley and McCrum<sup>38</sup> and Buckley<sup>39</sup>

Table 2. Thermomechanical data for polypropylene

Temperature	$\alpha_f^c$	Expansivity $\alpha_{\parallel}^c$ ( $10^{-5} \text{K}^{-1}$ )	$\alpha^a$
120	7.3	-0.8	4.5
240	9.7	-0.95	6.2
280	13.6	-1.0	9.8

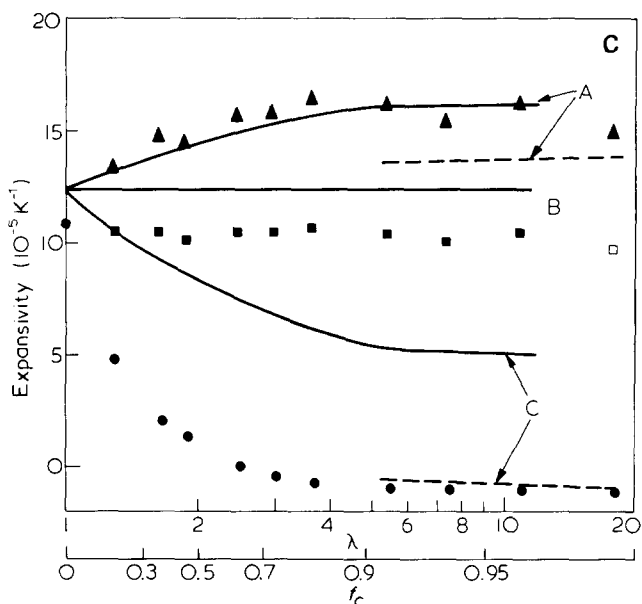
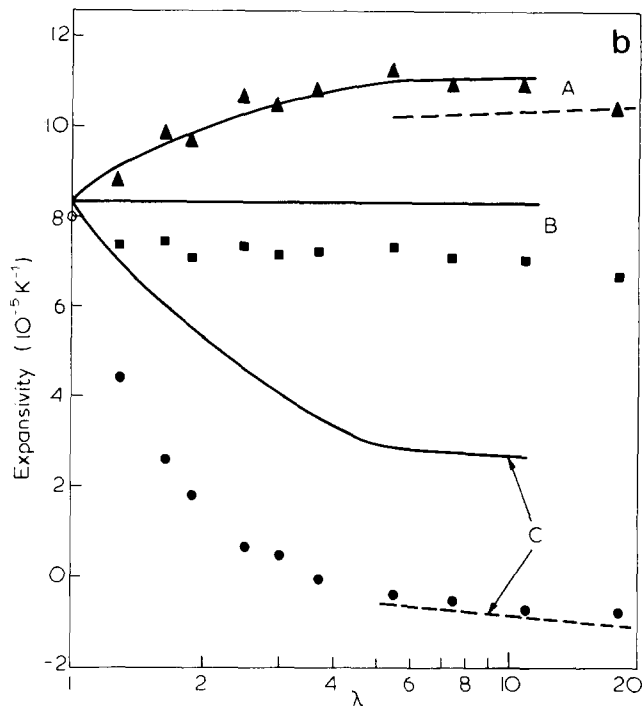
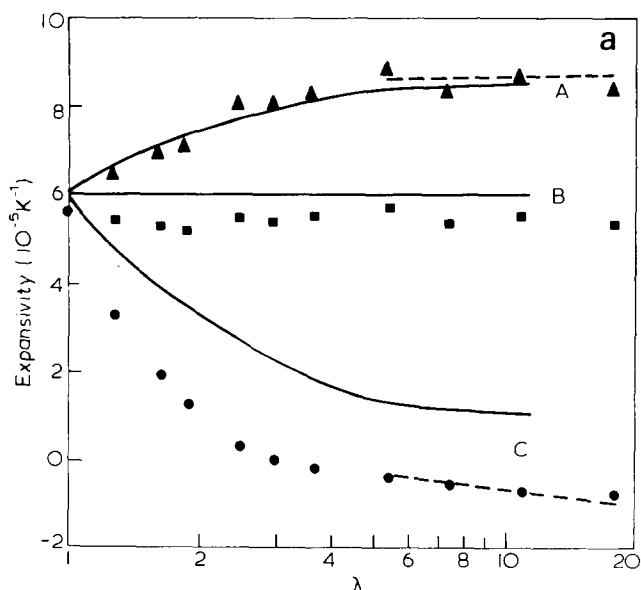


Figure 7. Linear thermal expansivities of drawn polyethylene as functions of draw ratio. a—120 K; b—170 K; c—280 K.

A:  $\alpha_{\perp}$ ; B:  $\alpha = \frac{1}{3}(2\alpha_{\perp} + \alpha_{\parallel})$ ; C:  $\alpha_{\parallel}$ . The points are the experimental data. Solid lines — theoretical curves according to linear mixture law (equations 3–5); Dashed lines — theoretical curves according to parallel-series model (equations 6–7)

on an annealed, single-crystal textured polyethylene sample at  $\lambda = 9$  yield a small positive value of  $\alpha_{\parallel}$  — in marked contrast to our result. This difference can probably be attributed to the absence of intercrystalline bridges in the annealed sample.

Turning now to temperature dependence from Figure 2 it can be seen that  $\alpha_{\perp}$  is not very sensitive to variation in the draw-ratio. Choosing the case  $\lambda = 5.5$  as an example, the temperature dependence can be correctly reproduced by either equation (3) or (6), Figure 8a, which indicates that  $\alpha_{\perp}$  is only weakly affected by intercrystalline bridges even at high draw ratio and that it simply follows the increase of  $\alpha^a$  and  $\alpha_f^c$  with temperature (Figure 6). The 5–15%

discrepancy between data and theory is not too surprising in view of the simplicity of the models and the uncertainty in some of the indirectly deduced input parameters, especially  $\alpha^a$  and  $E^a$ , both of which have strong temperature dependence.

$\alpha_{||}$  is more complicated. The low draw ratio curves (excepting  $\lambda < 2$ ) are dominated by the remarkable peak at 170 K and a quick drop in value (changing sign in some of the cases) at higher temperature (Figure 3). This is in total disagreement with equation (4), which would predict a monotonic increase with temperature, as clearly demonstrated by the example of  $\lambda = 2.5$  (Figure 8a). As previously mentioned, one might conjecture that a certain amount of intercrystalline bridges is present even at low draw ratio. Then the decrease in value of  $\alpha_{||}$  above 170 K can be attributed to the constraining effect of these crystalline bridges, which would become increasingly important above the transition at 145 K, when the stiffness of the expansive amorphous phase drops drastically in comparison with the crystalline phase.

The parallel-series model would have to be used for describing the expansivities at yet higher drawn ratio ( $\lambda \geq 5.5$ ). It is seen from Figure 8b that results for  $\alpha_{||}$  calculated from

equation (7) agree to within 20% with data. The observed monotonic decrease of  $\alpha_{||}$  with increasing temperature reflects the dominance of the negative expansivity  $\alpha_{||}^c$  throughout the temperature range.

Turning to PP, in principle the above analysis can be repeated by use of equations (3) to (7). But  $\alpha^a$ ,  $\alpha_{\perp}^c$  and  $\alpha_{||}^c$  cannot be reliably estimated over a temperature range and there is no data on  $\nu_f$ , so only an analysis of the draw ratio dependence at three temperatures: 120 K, 240 K – both below the glass transition at 260 K – and 280 K will be performed. The results as shown in Figures 9a-c have essentially the same features as those for PE. However, the discrepancy between theory and data on  $\alpha_{||}$  is considerably smaller than PE, which probably indicates a much smaller effect of intercrystalline bridges. This can also be seen from the fact that only at rather high draw ratio ( $\lambda \geq 8$ ) would  $\alpha_{||}$  assume negative values and become a monotonically decreasing function of temperature, both of which reflects the behaviour of  $\alpha_{||}^c$ .

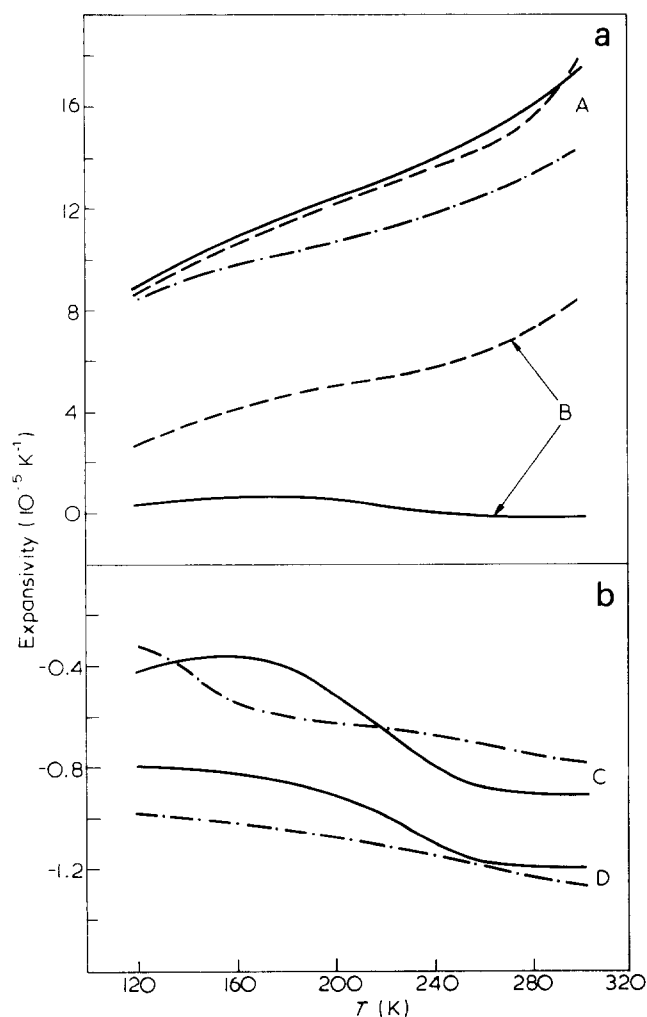
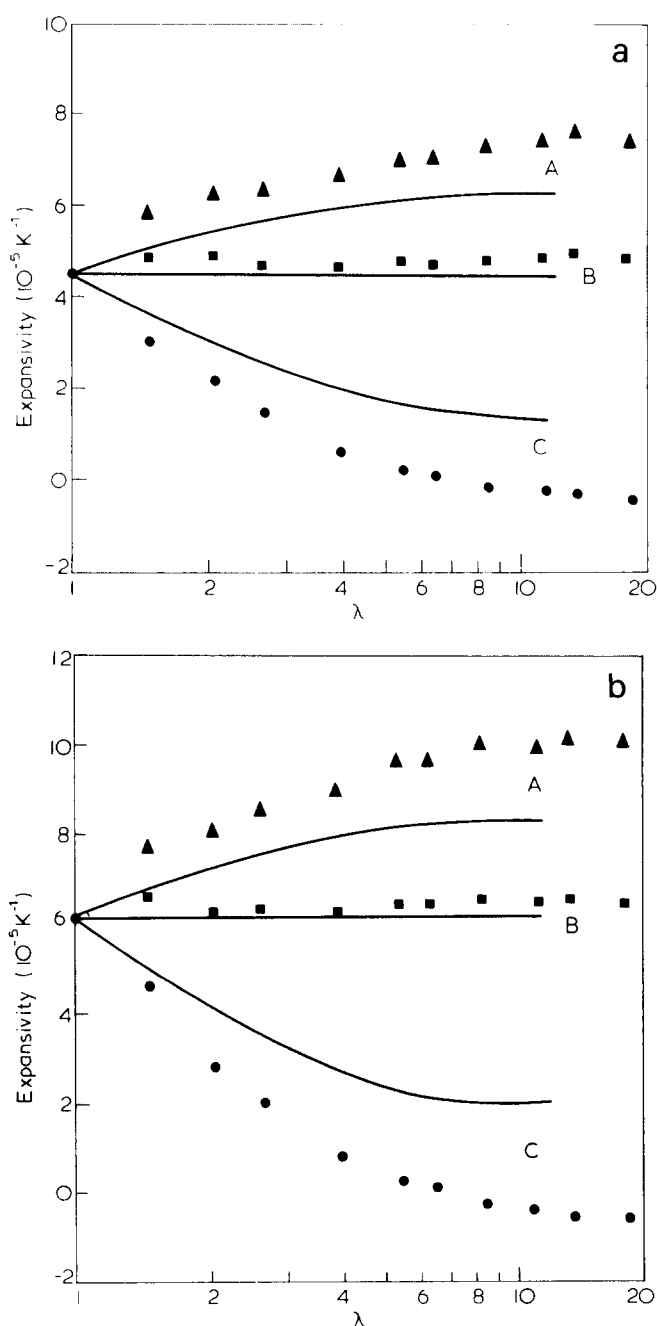


Figure 8 Temperature dependence of the linear thermal expansivities of drawn polyethylene, A:  $\alpha_{\perp}$ ,  $\lambda = 5.5$ ; B:  $\alpha_{||}$ ,  $\lambda = 2.5$ ; C:  $\alpha_{||}$ ,  $\lambda = 5.5$ ; D:  $\alpha_{||}$ ,  $\lambda = 18$ . — Data; - - - predictions according to linear mixture law (equations 3 and 4); - · - · - predictions according to parallel-series model (equations 5 and 6)



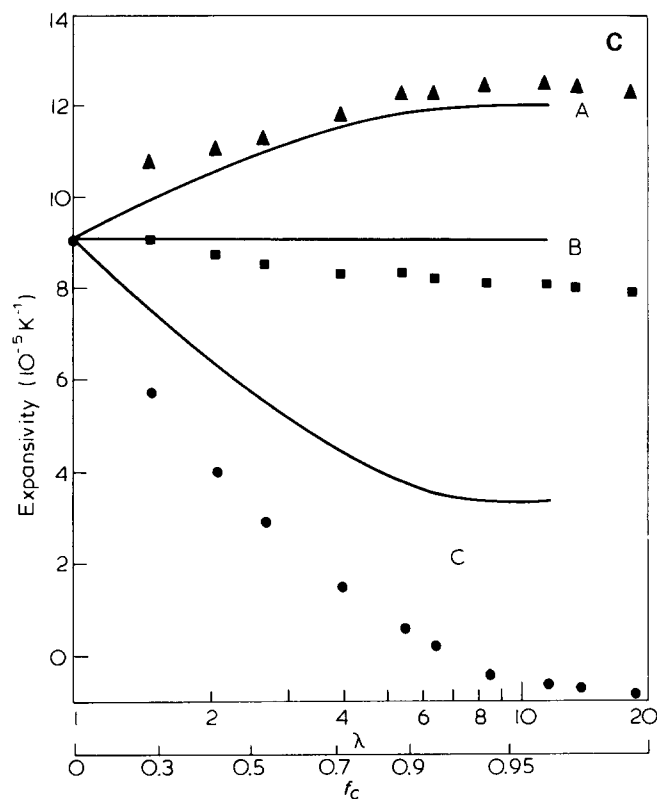


Figure 9 Linear thermal expansivities of drawn polypropylene as functions of draw ratio. a—120 K; b—240 K; c—280 K. A:  $\alpha_{\perp}$ ; B:  $\alpha = \frac{1}{2}(2\alpha_{\perp} + \alpha_{\parallel})$ ; C:  $\alpha_{\parallel}$ . The points are the experimental data. Solid lines — theoretical curves according to linear mixture law (equations 3-5); dashed lines — theoretical curves according to parallel-series model (equations 6 and 7)

## CONCLUSION

The above analysis shows that as far as  $\alpha_{\perp}$  is concerned the oriented polymer at all draw ratios may adequately be treated as a composite with partially aligned crystalline blocks embedded in an isotropic amorphous phase. On the other hand, the behaviour of  $\alpha_{\parallel}$  is very sensitive to the presence of intercrystalline bridges. For ultra-oriented samples  $\alpha_{\parallel}$  is largely independent of  $\lambda$ ; its value as a function of temperature can be estimated with reasonable accuracy ( $\sim 20\%$ ) on the basis of a parallel-series model if the volume fraction  $\nu_f$  of the intercrystalline bridges is known. However, neither of these two models is applicable to  $\alpha_{\parallel}$  at low draw ratio, for which the chain alignment of the crystalline blocks is not complete and yet a certain amount of intercrystalline bridges with unknown  $\nu_f$  is likely to be present. A realistic calculation would have to take both effects into account, and may depend on other details of the morphology as well. In this connection note that  $\alpha_{\parallel}$  of low-density PE drawn to  $\lambda = 4$  has been found<sup>40</sup> to have the startling room-temperature value of  $-5 \times 10^{-5}/\text{K}$ , which is even lower than  $\alpha_{\parallel}^c$  of PE by a factor of 4. Therefore considerable effort is still required for further elucidation of the underlying mechanism determining the expansivities.

## ACKNOWLEDGEMENT

The authors wish to thank British Petroleum Chemicals Ltd. for supplying Rigidex 50 polyethylene and to Hoechst Co. for supplying Hostalen PPK 1060 polypropylene.

## REFERENCES

- Hadley, D.W., Pinnock, P.R. and Ward, I.M. *J Mater Sci* 1969, **4**, 152
- Williams, T. *J Mater Sci* 1973, **8**, 59
- Gibson, A.G., Ward, I.M., Cole, B.N. and Parsons, B. *J Mater Sci* 1974, **9**, 1193
- Capaccio, G. and Ward, I.M. *Polymer* 1974, **15**, 233
- Capiati, N.J. and Porter, R.S. *J Polym Sci, Phys Ed* 1975, **13**, 1177
- Cansfield, D.L.M., Capaccio, G. and Ward, I.M. *Polym Eng Sci* 1976, **16**, 721
- Clark, E.S. and Scott, L.S. *Polym Eng Sci* 1974, **14**, 682
- Taylor, W.N. and Clark, E.S. *Polym Preprints* 1977, **18**, 332
- Weeks, N.E. and Porter, R.S. *J Polym Sci Phys Ed* 1974, **12**, 635
- Hansen, D. and Bernier, G.A. *Polym Eng Sci* 1972, **12**, 204
- Burgess, S. and Greig, D. *J Phys (C)* 1975, **8**, 1637
- Choy, C.L. and Greig, D. *J Phys (C)* 1977, **10**, 169
- Gibson, A.G., Greig, D., Sahota, M., Ward, I.M. and Choy, C.L. *J Polym Sci (Polym Lett Ed)* 1977, **15**, 183
- Choy, C.L., Luk, W.H. and Chen, F.C. *Polymer* 1978, **19**, 155
- Hellwege, K.H., Hennig, J. and Knappe, W., *Kolloid, Z. Z Polym* 1963, **188**, 121
- Kobayashi, Y. and Keller, A. *Polymer* 1970, **11**, 114
- Davis, G.T., Eby, R.K. and Colson, J.P. *J Appl Phys* 1970, **41**, 4316
- Stehling, F.C. and Mandelkern, L. *Macromolecules* 1970, **3**, 242
- Porter, R.S., Weeks, N.E., Capiati, N.J. and Krzewski, R.J. *J Thermal Analysis* 1975, **8**, 547
- Capiati, N.J. and Porter, R.S. *J Polym Sci, Phys Ed* 1977, **15**, 1427
- Hay, I.L. and Keller, A. *Kolloid-Z* 1965, **204**, 43
- Stein, R.S. and Rhodes, M.B. *J Appl Phys* 1960, **31**, 1873
- Peterlin, A. *Kolloid-Z* 1969, **233**, 857
- Fischer, E.W., Goddar, H. and Peiszcsek, W. *J Polym Sci (C)* 1971, **32**, 149
- Gibson, A.G., Davies, G.R. and Ward, I.M. *Polymer* 1978, **19**, 683
- Kavesh, S. and Schultz, J.M. *J Polym Sci (A-2)* 1970, **8**, 243
- Rosen, B.W. and Hashin, Z. *Int J Eng Sci* 1970, **8**, 157
- Barham, P.J. and Arridge, R.G.C. *J Polym Sci, Phys Ed* 1977, **15**, 1177
- Gibbons, D.F. *Phys Rev* 1958, **112**, 136
- Pietralla, M. *Kolloid-Z* 1976, **254**, 249
- Samuels, R.J. 'Structured Polymer Properties' Wiley, NY, 1974, pp 117
- Beck, D.L., Hiltz, A.A. and Knox, J.R. *SPE Transactions* 1963, **3**, 279
- Odajima, A. and Maeda, M. *J Polym Sci (C)* 1966, **15**, 55
- Sakurada, I., Ito, T. and Nakamae, K. *J Polym Sci (C)* 1966, **15**, 75
- Holliday, L. 'Structure and Properties of Oriented Polymers' (Ed. I.M. Ward) Applied Science Publishers Ltd, London, 1975, pp 242
- Clements, J., Jakeways, R. and Ward, I.M. *Polymer* 1978, **19**, 639
- Gray, R.W. and McCrum, N.G. *J Polym Sci (A-2)* 1969, **7**, 1329
- Buckley, C.P. and McCrum, N.G. *J Mater Sci* 1973, **8**, 1123
- Buckley, C.P. *J Mater Sci* 1974, **9**, 100
- Kim, B.H. and De Batist, R. *J Polym Sci Lett Ed* 1973, **11**, 121
- Mandelkern, L., Posner, A.S., Diorio, A.F. and Roberts, D.E. *J Appl Phys* 1961, **32**, 1509